Journal of Engineering Science and Technology
23rd EURECA 2025 Special Issue February (2026) 133 - 154


# THE ELECTROCHEMICAL IMPEDANCE PERFORMANCE OF EPOXY AND POLYESTER COMPOSITE COATINGS FOR CORROSION PROTECTION ON MILD STEEL

TAN LAI HIN[1], SACHIN SHARMA ASHOK KUMAR[1,2,3,*], K. RAMESH[3,4], S. RAMESH[3,5]

[1] School of Engineering, Faculty of Innovation & Technology, Taylor's Lakeside Campus, Subang Jaya, Selangor, Malaysia
[2]Mechanical Engineering Department, Faculty of Engineering, Lincoln University College, 47301, Petaling Jaya, Selangor, Malaysia
[3]Centre for Ionics University of Malaya, Department of Physics, Faculty of Science, Universiti Malaya, 50603 Kuala Lumpur, Malaysia
[4]Department of Physical Sciences, Saveetha School of Engineering, Saveetha University (SIMATS), Chennai, India
[5]Department of Chemistry, Saveetha School of Engineering, Institute of Medical and Technical Science, Saveetha University, Chennai 602105, Tamil Nadu, India
*Corresponding Author: sachin.sharma@taylors.edu.my

## Abstract

This study investigates the performance of epoxy-based composite coatings for corrosion protection by formulating hybrid resin systems with varied epoxy-to-polyester ratios. This research aims to evaluate how the blending these resins, combined with polydimethylsiloxane (PDMS) as a hydrophobic modifier, influences the coating properties. Six coating samples were synthesized, comprising two reference systems (100% epoxy and 100% polyester) and four hybrid formulations (8E2PE, 6E4PE, 4E6PE and 2E8PE). Isophorone diamine (IPDA) was incorporated as a crosslinking agent to enhance the interaction between epoxy and polyester phases and ensure strong interfacial bonding with PDMS. The fabricated coatings were characterized via Electrochemical Impedance Spectroscopy (EIS), Cross Hatch Test (CHT), Water Contact Angle (WCA) analysis and Fourier Transform Infrared Spectroscopy (FTIR). The results revealed that the 8E2PE coating sample exhibited the most balanced and superior performance, with high impedance modulus ($|Z|_{0.01\,Hz}$) values, excellent adhesion rated 5B under ASTM D3359 Method B and a contact angle of approximately 83.55°. FTIR analysis confirmed the presence of crosslinked structures and characteristic bonds corresponding to the functional components. In overall, these findings affirm the efficacy of epoxy–polyester hybrid systems as a promising route towards the advanced corrosion-protective coatings.

Keywords: Barrier performance, Corrosion resistance, Crosslinking, Electrochemical stability, Hydrophobic.

## 1. Introduction

Corrosion remains a persistent and critical challenge across a wide range of industrial sectors, undermining the structural integrity, operational safety, and economic viability of metallic components. It is fundamentally characterized by the electrochemical degradation of materials through interactions with environmental factors such as moisture, oxygen, and chloride ions. This gradual deterioration compromises infrastructure durability, necessitates frequent maintenance, and contributes to unplanned operational downtimes and material losses. The global economic impact of corrosion is substantial, with estimated costs exceeding USD 2.5 trillion annually, equivalent to approximately 3 to 4 percent of the world's gross domestic product, thereby reinforcing the imperative for effective corrosion mitigation strategies as highlighted by Koch et al. [1].

Among the various approaches to corrosion prevention, the use of protective coatings has emerged as one of the most efficient and widely adopted methods. These coatings act as physical and chemical barriers that impede the diffusion of aggressive species to the underlying metal substrate. In particular, polymeric coatings have gained significant attention due to their application versatility, cost-efficiency, and capacity to form continuous, adherent films. Epoxy-based coatings, in this context, have been extensively utilized owing to their exceptional adhesion to metallic surfaces, chemical resistance, and mechanical robustness. When adequately crosslinked using suitable curing agents, epoxy matrices form tightly interlinked three-dimensional networks that hinder the permeation of moisture and corrosive ions, thereby enhancing the longevity and protection of the coated system, as reported by Yang et al. [2] and Huang et al. [3].

Despite these advantages, conventional epoxy coatings are not devoid of limitations. Their intrinsic brittleness, proneness to microcrack formation under mechanical deformation, and inadequate flexibility pose significant challenges in environments subjected to thermal and mechanical stress. To address these deficiencies, recent research has focused on structural modifications of epoxy systems through resin blending, curing agent optimization, and the incorporation of functional additives. A promising strategy involves the integration of polyester resins with epoxy matrices to form hybrid systems that benefit from the complementary properties of both polymers. Polyester, being a thermosetting resin with good film-forming ability and inherent hydrophobic nature, imparts improved flexibility and water repellency to the coating, thereby reducing moisture ingress and enhancing surface smoothness, as demonstrated in the work of Adnan et al. [4].

Additionally, the incorporation of hydrophobic surface modifiers such as polydimethylsiloxane (PDMS) has been explored to further elevate the moisture resistance of the coating system. PDMS, due to its flexible siloxane backbone and low surface energy, migrates to the outer surface of the coating, forming a hydrophobic interface that effectively repels water molecules. This modification not only mitigates capillary water transport but also contributes to a smoother and more defect-resistant surface. The selection of curing agents plays an equally critical role in defining the crosslinking architecture and final performance of the composite coating. Aliphatic amines such as isophorone diamine (IPDA) are commonly employed in epoxy-rich systems to achieve high crosslink density, while polyisocyanate-based compounds (NCO-functional groups) are more compatible

with polyester formulations due to their reactivity with hydroxyl groups, facilitating robust network formation [5].

In the pursuit of durable and multifunctional protective coatings, contemporary research efforts are increasingly focused on developing synergistic multi-resin systems that transcend the limitations of single-polymer formulations. By strategically tailoring the ratio of epoxy to polyester, selecting optimal curing agents, and integrating hydrophobic modifiers such as PDMS, it becomes feasible to engineer composite coatings with enhanced corrosion resistance, improved mechanical flexibility, and long-term stability under aggressive environmental conditions. As demonstrated by Kumar et al. [6] and Peng et al. [7], this integrative design approach offers promising avenues for the development of next-generation protective coatings.

To evaluate the effectiveness of such advanced coatings, a suite of analytical and electrochemical techniques is employed. Fourier-transform infrared spectroscopy (FTIR) provides insight into the molecular interactions and chemical bonding within the composite matrix. Water contact angle (WCA) measurements quantify the surface wettability and hydrophobic characteristics, offering an indirect indication of water barrier performance. Electrochemical impedance spectroscopy (EIS) is used to assess the electrochemical barrier properties and durability of the coating system over prolonged immersion in saline environments, thereby simulating real-world exposure conditions [8].

The present study is designed on the hypothesis that an optimized combination of epoxy and polyester resins, reinforced with PDMS and selected curing chemistries, can produce a composite coating with superior protective capabilities. This research aims to systematically investigate how variations in resin ratios, crosslinking agents, and hydrophobic additives influence the microstructural integrity, surface morphology, and electrochemical behaviour of the resulting coatings. The findings are expected to contribute valuable knowledge toward the design of high-performance, corrosion-resistant polymeric coatings suitable for application in demanding industrial environments.

## 2. Experimental Materials and Methods

### 2.1. Materials

The formulation of the epoxy-based composite coatings in this study was achieved using a carefully selected combination of polymeric resins, hydrophobic modifiers, and curing agents, each chosen for its distinct physicochemical properties relevant to corrosion protection. The primary resin used was a bisphenol-A type epoxy resin (Eponex 1510), selected for its excellent mechanical strength, superior adhesion to metallic substrates, and high chemical resistance. With a viscosity of approximately 2000 cP at 25 °C and a density of 1.15 g/cm³, Eponex 1510 can form dense, highly crosslinked networks that effectively resist the diffusion of moisture and ions, thereby enhancing the coating's barrier properties [9, 10].

To improve the coating's flexibility and processability, a saturated polyester resin with a lower viscosity of approximately 850 cP at 25 °C was incorporated as a co-resin in various proportions. Polyester offers advantages in terms of ease of handling, elasticity, and film-forming capability, contributing to the mechanical toughness of the final coating [11]. However, due to the hydrolytic vulnerability of ester linkages in aqueous and saline environments, polyester was not used

independently but instead blended with epoxy to explore synergistic improvements in overall performance. This blending strategy aimed to combine the impermeability and chemical resistance of epoxy with the toughness and surface smoothness imparted by polyester, consistent with previous studies on miscibility and crosslink network design in hybrid polymer systems [12].

To further enhance surface properties and moisture resistance, PDMS was included in all formulations as a hydrophobic surface modifier. PDMS is well known for its low surface energy (~21 mN/m), high thermal stability, and flexibility, with a density of 0.97 g/cm³ [13]. During the curing process, PDMS migrates toward the coating-air interface, forming a water-repellent layer that reduces surface wettability and inhibits water absorption and crack propagation. Its incorporation into hybrid matrices has been shown to improve long-term corrosion resistance by retarding ionic transport across the coating barrier [14].

Two distinct curing systems were used to accommodate the respective resin chemistries. Epoxy-rich formulations (10E, 8E2PE, 6E4PE) were cured with EPIKURE 3388, a cycloaliphatic amine-based curing agent known for its room-temperature reactivity and minimal yellowing. This agent was used at a fixed ratio of 24 parts per 100 parts epoxy resin by weight to ensure complete crosslinking and robust film integrity [15]. In contrast, polyester-dominant systems (10PE, 2E8PE, 4E6PE) employed a polyisocyanate (NCO-based) curing agent. The required amount of NCO was calculated based on the hydroxyl value of the polyester resin using the following formula:

$$\text{Amount of isocyanate} = \frac{\text{Solid weight of polyester} \times \text{Molecular weight of NCO} \times \text{OH value}}{\text{Molecular weight of OH} \times \text{NCO value}} \quad (1)$$

This stoichiometric balance ensures adequate crosslinking while avoiding excess unreacted isocyanate, which could result in brittle films with reduced aging stability [16].

To further reinforce interphase compatibility between epoxy and polyester domains in blended systems, IPDA was introduced as a secondary crosslinking agent. IPDA, a cycloaliphatic diamine with a viscosity of approximately 85 cP at 25 °C, provides high reactivity and facilitates the formation of interpenetrating polymer networks (IPNs) [17]. Its presence enhances matrix cohesion, reduces the risk of phase separation, and improves film uniformity. Previous studies have demonstrated that the inclusion of IPDA in multi-resin systems significantly improves corrosion resistance and mechanical performance through better crosslinking at the molecular level [18]. All chemical components used in the formulations were utilized as received, without further purification.

## 2.2. Preparation of coatings

The preparation of epoxy-based composite coatings involved a systematic combination of resins, functional modifiers, and curing agents to produce homogeneous and stable systems. Seven distinct coating compositions were prepared by adjusting the weight ratios of epoxy (Eponex 1510) to saturated polyester resin. These formulations included 10E, 8E2PE, 6E4PE, 4E6PE, 2E8PE, and 10PE. Each blend incorporated five weight percent of hydroxyl-terminated PDMS as a hydrophobic additive to enhance surface moisture resistance. The objective of this formulation approach was to investigate the influence of resin composition, crosslinking chemistry, and hydrophobic modification on corrosion protection and coating performance.

The required amounts of epoxy and polyester were accurately measured using an analytical balance and placed into a clean, dry 250 millilitres beaker. Mixing was performed using a mechanical stirrer at 500 revolutions per minute for fifteen minutes to ensure complete homogeneity. PDMS was introduced slowly while maintaining continuous stirring for an additional ten minutes to achieve uniform distribution throughout the resin matrix. The curing agent was selected based on the dominant resin in each system. Epoxy-based compositions including 10E, 8E2PE, and 6E4PE were cured using EPIKURE 3388, added at twenty-four parts per one hundred parts of epoxy resin by weight, based on stoichiometric calculations. For formulations where polyester was the main component, such as 4E6PE, 2E8PE, and 10PE, a polyisocyanate curing agent containing isocyanate functional groups was used. The required mass of this curing agent was calculated according to the hydroxyl number of the polyester resin to ensure balanced reactivity and avoid excessive isocyanate that may lead to brittleness.

In blends containing both epoxy and polyester, IPDA was added as a secondary crosslinking agent. It was introduced at a ratio of ten parts per one hundred parts of total resin content to promote chemical compatibility between the two resin phases and minimize the risk of phase separation. After adding the curing agent and IPDA, the mixture was stirred gently at 300 revolutions per minute for five minutes. This step minimized air entrapment and ensured thorough incorporation of all ingredients. The final coating mixtures were then applied to pre-treated mild steel substrates using a flat brush application method, targeting a wet film thickness between 150 and 180 micrometres. The coated panels were allowed to cure under ambient laboratory conditions at approximately 25 ℃ and a relative humidity of 50 to 60 percent for seven days.

Polyester-dominant systems that used polyisocyanate curing agents underwent an additional post-curing stage in a convection oven at 60 ℃ for two hours. This additional step accelerated the reaction and enhanced mechanical strength. Once fully cured, all coated specimens were stored in desiccators until they were subjected to further characterization and performance testing. This stepwise and controlled preparation method ensured reproducibility and uniformity across all coating formulations, enabling a consistent basis for subsequent performance evaluations. The illustrated in Table 1 are the compositions of all the prepared coating systems along with their corresponding designation and the average thickness of dry coating film after being applied on the substrate surface. Also, in Fig. 1 illustrates the coated microscope slides (metal) substrates for each corresponding sample respectively and Fig. 2 presents the compositions of all the formulated coating systems, including their respective designations and the average dry film thickness measured after application onto the glass substrate.

**Table 1. The composites of the coating samples and the corresponding designations.**

| Samples (g) | Sample code | Curing Agent (g) | PDMS (g) | IPDA (g) |
|---|---|---|---|---|
| 10 Epoxy | 10E | 2.4 (EPI-KURE 338) | 0.1 | - |
| 10 Polyester | 10PE | 3.72 (NCO) | 0.1 | - |
| 2 Epoxy:8 Polyester | 2E8PE | 2.98 (NCO) | 0.1 | 0.2 |
| 4 Epoxy:6 Polyester | 4E6PE | 2.23 (NCO) | 0.1 | 0.4 |
| 6 Epoxy:4 Polyester | 6E4PE | 1.44 (EPI-KURE 338) | 0.1 | 0.6 |
| 8 Epoxy:2 Polyester | 8E2PE | 1.92 (EPI-KURE 338) | 0.1 | 0.8 |


**Fig. 1. The coatings samples prepared on metal plate in this study.**

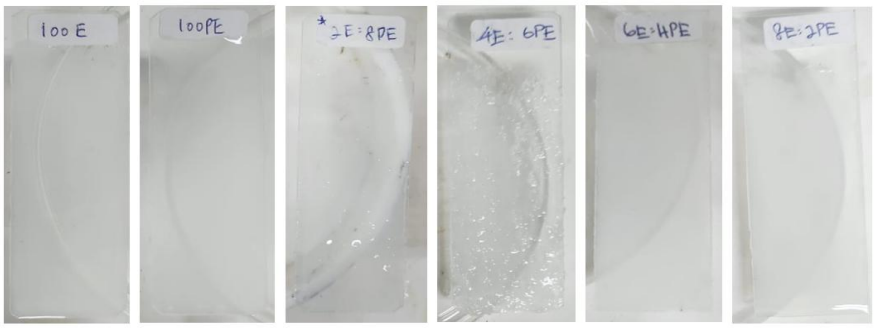


**Fig. 2. Coating on glass substrates.**

## 3. Characterization

### 3.1. Fourier-transform infrared spectroscopy (FTIR)

Fourier Transform Infrared Spectroscopy (FTIR) was employed to analyse the chemical structure and functional groups present in the formulated coatings. The analysis was conducted using a Thermo Fisher Scientific ATR-Nicolet iS10 spectrometer (USA), a reliable instrument known for its high sensitivity in identifying molecular vibrations. Spectral data were collected in transmission mode over a wavenumber range of 4000 to 500 $cm^{-1}$, with a resolution of 4.0 $cm^{-1}$, and each sample spectrum was obtained through the accumulation of 32 scans to ensure clarity and accuracy. This technique enabled the detection of characteristic absorption peaks corresponding to various functional groups, such as hydroxyl, carbonyl, ether, and siloxane linkages, thereby confirming the structural composition and molecular interactions within the epoxy, polyester, and PDMS-modified coatings [19]. The FTIR analysis provided essential insights into the degree of polymer crosslinking and the chemical compatibility of the blended resin systems, supporting prior studies that highlight the effectiveness of FTIR in evaluating curing behaviour and network formation in polymeric coatings [20].

### 3.2. Water contact angle (WCA) measurements

Contact angle measurements were performed using an Optical Contact Angle (OCA) 15EC device from Data Physics Instruments GmbH (Germany), which was equipped with a CCD camera and a digital adapter to accurately capture the wettability behaviour of the composite coatings, both with and without the addition

of PDMS. To assess surface hydrophobicity, five droplets of distilled water, each with a volume of 5 µL, were carefully dispensed at various positions on the coated glass substrates. The static contact angles were measured at each point. To minimize the influence of droplet kinetic energy and ensure accurate readings, the needle tip was positioned in close proximity to the sample surface during droplet deposition. For each coating, five measurements were taken, and the highest value showing a margin of error of less than 1° was reported. All measurements were recorded in real time through image capture, providing clear visual evidence of the droplet behaviour on the coating surface [21].

### 3.3. Cross hatch test (CHT)

The CHT was conducted to evaluate the adhesion strength of the coating to the substrate, following the ASTM D3359 B standard. An Elcometer 107 crosshatch cutter was gently applied to the coated surface, and under light pressure, a series of parallel cuts approximately 20 mm in length were made through the coating layer. To create a lattice pattern, a second set of cuts was performed perpendicular to the first set by rotating the cutter 90°, forming a grid on the coating surface. Any loose flakes or fragments resulting from the cutting were carefully removed using a clean brush to ensure a clear assessment area. A specialized adhesive tape was then firmly applied over the centre of the lattice, with pressure applied using a standard pencil eraser to ensure full contact between the tape and the coating surface. After allowing the tape to adhere for two minutes, it was peeled off in a single, smooth motion at a 180° angle to test the coating's resistance to detachment. The resulting lattice area was then examined under a phone camera, where detailed images of the cuts were captured to analyse the coating’s adhesion performance for each sample [22].

### 3.4. Electrochemical impedance spectroscopy (EIS)

EIS was utilized to assess the corrosion resistance and barrier performance of the developed nanocomposite coatings. A standard three-electrode cell setup was employed, in which the coated sample served as the working electrode, exposing an area of 3 cm² to a 3.5 wt.% NaCl solution. A saturated calomel electrode (SCE) acted as the reference electrode, while a pyrolytic graphite electrode was used as the counter electrode. To reduce the influence of external electromagnetic interference and ensure measurement accuracy, all experimental components and electrical connections were housed within a Faraday cage during testing. The EIS measurements were conducted over an immersion period of 60 days to monitor the long-term electrochemical stability of the coatings. A Gamry PCI4 G300 potentiostat (Warminster, PA, USA) was employed to perform the tests, operating within a frequency range of 100 kHz to 10 MHz at open circuit potential (OCP), using a sinusoidal AC signal with a 10-mV root mean square (rms) amplitude. The resulting impedance data were processed and analysed using Gamry Echem Analyst software, Version 6.03 (Warminster, PA, USA), to interpret the coatings' degradation behaviour and evaluate their protective performance over time [23].

## 4. Results and Discussion

### 4.1. FTIR

The FTIR was employed to analyse the chemical structure of the developed epoxy-based composite coatings and confirm the successful incorporation of functional

groups from each resin and additive component. Across all samples, characteristic absorption bands associated with the epoxy resin backbone were observed as shown in Fig. 3. Notably, strong absorption peaks in the region of 910–915 $cm^{-1}$ were attributed to the epoxide ring deformation vibrations, indicating the presence of unreacted epoxy groups, particularly in the 10E and 8E2PE samples. The intensity of these peaks diminished in samples with higher polyester content, such as 10PE and 2E8PE, suggesting more extensive crosslinking with curing agents or a dilution effect due to resin ratio.

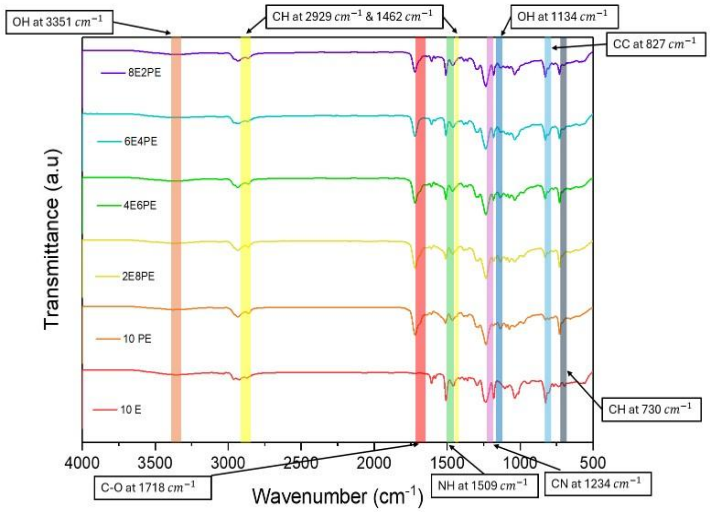


**Fig. 3. FTIR spectra for all samples.**

Furthermore, the broad absorption band around 3400 $cm^{-1}$, evident in all coatings, was assigned to the stretching vibrations of hydroxyl (–OH) groups. This peak is commonly linked to the secondary alcohols formed during the ring-opening reaction of epoxides with amines like IPDA. The appearance of this feature in samples containing both epoxy and polyester indicates successful crosslinking and interaction between the two resins. Additionally, peaks near 1720–1735 $cm^{-1}$ were attributed to the stretching vibrations of carbonyl (C=O) groups, a distinctive marker of polyester content. These bands were particularly pronounced in the 10PE and 2E8PE formulations, confirming the increasing presence of ester linkages and the integration of polyester in the hybrid networks.

The presence of PDMS in the formulations was also confirmed by the appearance of absorption bands in the range of 1000–1100 $cm^{-1}$, typically associated with Si–O–Si stretching vibrations. These peaks were especially distinct in the 8E2PE and 6E4PE samples, where PDMS was actively incorporated to enhance hydrophobicity. This confirms that PDMS was successfully embedded within the coating matrix, potentially improving moisture barrier performance. Moreover, minor peaks detected around 1258 $cm^{-1}$ were linked to C–N stretching vibrations from aliphatic amines, originating from curing agents like EPIKURE 3388 and IPDA. Their presence across the epoxy-dominant samples supports the formation of amine-cured epoxy networks.

Overall, the FTIR spectra provided compelling evidence for the coexistence of epoxy, polyester, and PDMS components in the hybrid coatings, as well as the formation of key functional linkages through curing and crosslinking reactions. These spectral features align with findings from Kumar et al. [6], who reported similar band assignments when characterizing multi-resin polymer coatings. The ability to detect such chemical signatures confirms that the structural integrity and compositional goals of each coating were successfully achieved, validating the intended formulation strategy.

## 4.2. WCA

WCA measurements were conducted to evaluate the surface wettability and hydrophobic performance of the epoxy composite coatings as shown in Fig. 4. The contact angle, defined as the angle formed between the tangent to a water droplet and the solid surface, serves as an indicator of the coating's resistance to moisture accumulation and its potential for corrosion prevention. Generally, higher contact angles denote enhanced surface hydrophobicity and lower wettability, both of which are desirable characteristics for protective coatings in aggressive environments.

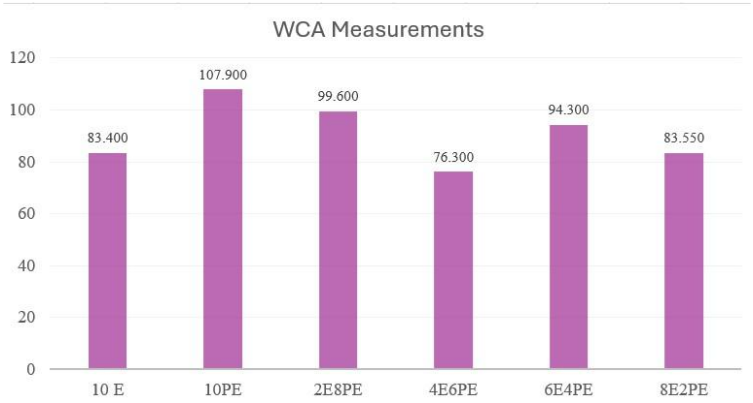


**Fig. 4. WCA measurements for all the coating samples.**

The polyester-based coating (10PE) exhibited the highest contact angle of 107.9°, reflecting excellent hydrophobic behaviour. This result is consistent with the inherently non-polar chemical structure of polyester chains, which contain limited hydroxyl and carboxyl groups, thereby reducing the surface energy of the film. The incorporation of polydimethylsiloxane (PDMS), a siloxane-based surface modifier known for its methyl-terminated backbone, likely further contributed to this performance. PDMS segments preferentially migrate to the surface during curing, resulting in a low-energy, hydrophobic outer layer. These findings align with the observations of Neves et al. [24] who reported that PDMS-modified coatings commonly achieve WCA values above 100°, indicative of superior moisture repellency and limited surface wetting.

The hybrid formulation 2E8PE also recorded a high WCA of 99.6°, affirming that polyester-dominant matrices, even when partially blended with epoxy, can maintain effective hydrophobicity when combined with siloxane additives. Despite containing 20% epoxy resin, the matrix retained low surface polarity, suggesting

that PDMS distribution and surface enrichment played a decisive role in repelling water. Notably, the 6E4PE sample demonstrated a WCA of 94.3°, which exceeded that of the pure epoxy system (10E, 83.4°). This enhancement may be attributed to the synergistic interplay between the moderately balanced resin ratio and PDMS phase migration to the surface. Ramos et al. [25] reported similar surface reconstruction behaviour in hybrid coatings, whereby PDMS-rich domains self-assemble at the air–coating interface, forming a hydrophobic barrier layer.

The 8E2PE and 10E samples showed comparable WCA values of 83.55° and 83.4°, respectively. These moderate contact angles are characteristic of epoxy-based coatings that possess both hydrophobic aromatic backbones and polar moieties such as hydroxyl and ether groups. Although these functional groups contribute to the structural rigidity and mechanical integrity of the coating, they also introduce sites for hydrogen bonding with water molecules, thereby reducing overall surface hydrophobicity. Nonetheless, the inclusion of PDMS in both formulations appeared to mitigate this limitation to some extent by maintaining contact angles above 80°, consistent with findings by Pistone et al. [26], who reported that PDMS-functionalized epoxy films exhibit suppressed water affinity despite their polar content.

In contrast, the 4E6PE formulation exhibited the lowest WCA of 76.3°, suggesting diminished hydrophobicity. This reduction may result from poor miscibility between epoxy and polyester phases at this specific composition, leading to heterogeneous surface morphology and incomplete PDMS migration. The possible presence of microphase-separated regions enriched with polar functionalities (e.g., unreacted hydroxyl or ester groups) may have increased the surface energy and promoted stronger water adhesion. As supported by prior work from Huang et al. [3], surface exposure of polar domains significantly enhances wettability, undermining the hydrophobic barrier function of protective coatings.

Collectively, the WCA data emphasize that high surface hydrophobicity is not inherently achieved through epoxy-rich compositions but rather through a careful balance of polymer chemistry, phase compatibility, and surface modifier distribution. Formulations such as 2E8PE and 6E4PE demonstrate that polyester-dominant matrices, when synergized with PDMS, offer optimal wettability control. In contrast, coatings with excessive epoxy content (e.g., 10E, 8E2PE) exhibit reduced contact angles despite their robust network structures. These findings underline the importance of interfacial design in promoting water repellence, a critical factor in limiting water permeation and delaying the initiation of corrosion-related electrochemical reactions.

## 4.3. CHT

The adhesion behaviour of the epoxy composite coatings was systematically assessed using the Cross Hatch Test (CHT) in accordance with ASTM D3359 Method B as shown in Fig. 5. This standardized procedure evaluates the mechanical integrity and interfacial bonding of coatings through the application of a lattice incision followed by tape pull-off. Adhesion quality is classified on a scale from 0B to 5B, where higher ratings denote superior film-substrate interaction and cohesive strength under mechanical stress. The 10E coating received a 5B rating, indicating excellent adhesion with no visible detachment or flaking. This result reflects a continuous, well-cured polymer network with strong interfacial

anchorage to the steel substrate. The dense crosslinked structure formed during curing likely facilitates enhanced bonding through both chemical and mechanical interactions. Kumar et al. [6] reported that such network structures suppress interfacial delamination by minimizing stress accumulation and improving compatibility at the coating–metal interface.

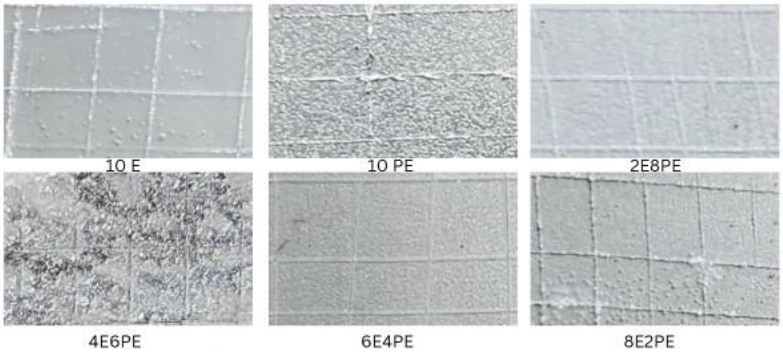


**Fig. 5. Adhesion performance of the coatings.**

Similarly, coatings 2E8PE, 6E4PE, and 8E2PE also achieved 5B ratings. These outcomes suggest that, despite compositional variations, the formulations exhibit sufficient phase uniformity and cohesive film formation to withstand mechanical peeling. The presence of PDMS in these systems may contribute to interfacial stress relaxation and enhanced film flexibility, thereby maintaining adhesion stability. According to Qi et al. [27], the incorporation of PDMS can improve film elasticity and reduce the formation of brittle interphases, which supports durable mechanical performance even under stress. The 10PE sample was rated at 3B, where partial removal of the coating film along the scribed edges was observed. The reduced adhesion can be linked to the inherent limitations of the polyester matrix, which lacks strong polar functional groups required for robust interaction with metallic substrates. In addition, its relatively lower crosslinking potential may result in weaker cohesive strength, making the film more susceptible to peeling during mechanical evaluation. This observation is consistent with the findings of Motlatle et al. [28], who emphasized that polyester systems generally require modification or blending to achieve adequate substrate adhesion.

Among all samples, the 4E6PE coating demonstrated the weakest adhesion performance, with a rating of 2B. Notable flaking and partial detachment suggest internal film discontinuities, likely due to resin incompatibility or poor phase homogeneity during curing. The observed failure mode may arise from insufficient epoxy content to establish a fully interconnected polymer network, resulting in void formation or weak interphase domains. Zhang et al. [29] highlighted that suboptimal resin blending often leads to heterogeneous microstructures that exhibit reduced mechanical resilience under localized stress.

Overall, the CHT results underscore the influence of formulation balance, curing behaviour, and network compatibility on adhesion performance. Coatings that demonstrated stable bonding behaviour exhibited uniform curing, efficient stress distribution, and coherent phase morphology. In contrast, those with weaker adhesion suffered from structural discontinuities and reduced cohesive forces. These findings

affirm that careful control of composition and curing dynamics is essential in engineering high-performance coatings for long-term protective applications.

## 4.4. EIS

The Day 1 electrochemical impedance spectroscopy (EIS) results serve as a foundational benchmark for assessing the initial corrosion protection behaviour of the epoxy-polyester composite coatings in a simulated 3.5 wt.% NaCl environment as shown in Fig. 6. The Bode plot reveals marked differences in impedance response among the tested formulations, with the 10E coating comprising entirely epoxy resin exhibiting the highest ($|Z|_{0.01\,Hz}$), exceeding $10^9\,\Omega\cdot cm^2$. This superior impedance reflects excellent dielectric properties and a highly compact, crosslinked matrix that effectively impedes ionic conduction and moisture penetration. Such behaviour aligns with findings reported by Kumar et al. [6], where densely packed epoxy networks were shown to significantly delay electrolyte diffusion due to the absence of microdefects and the tortuosity of the polymer network.

The polyester-based reference coating, 10PE, also demonstrated appreciable impedance values on the order of $10^8\,\Omega\cdot cm^2$, likely attributable to its intrinsic hydrophobic character and the incorporation of polydimethylsiloxane (PDMS), which acts to lower surface energy and enhance moisture repellence. These properties result in an initially robust barrier, as supported by Qi et al. [27], who observed that PDMS-modified systems effectively suppressed water ingress in polymer matrices due to surface restructuring and microphase segregation.

Among the hybrid compositions, the 2E8PE sample emerged as a particularly effective barrier, with impedance levels comparable to 10PE. This performance may be linked to favourable phase compatibility between the polyester and minor epoxy components, enabling the formation of a cohesive film with sufficient hydrophobicity and intermediate rigidity. Conversely, the 8E2PE and 4E6PE formulations exhibited lower impedance values, which likely result from phase separation, incomplete crosslinking, or morphological irregularities such as microvoids or interfacial defects. As highlighted by Motlatle et al. [28], these structural discontinuities act as preferential sites for electrolyte transport, accelerating coating degradation even during early exposure.

The Nyquist plots provide additional insight into interfacial charge transfer resistance and coating capacitance. All formulations displayed characteristic capacitive semicircles, indicative of a dominant barrier-type response. The 10E coating featured the largest arc diameter (Plot a), reflecting its high polarization resistance and well-established dielectric shielding. The arc's displacement from the origin further reinforces the integrity of the barrier layer, suggesting limited ionic exchange at the coating–electrolyte interface. This response is consistent with polymeric coatings exhibiting intact film morphology and high resistance to electrolyte penetration, as noted by Huang et al. [3]. Hybrid and polyester-rich systems such as 2E8PE and 10PE exhibited slightly reduced but still substantial arc diameters, further supporting their moderate-to-strong resistance capabilities.

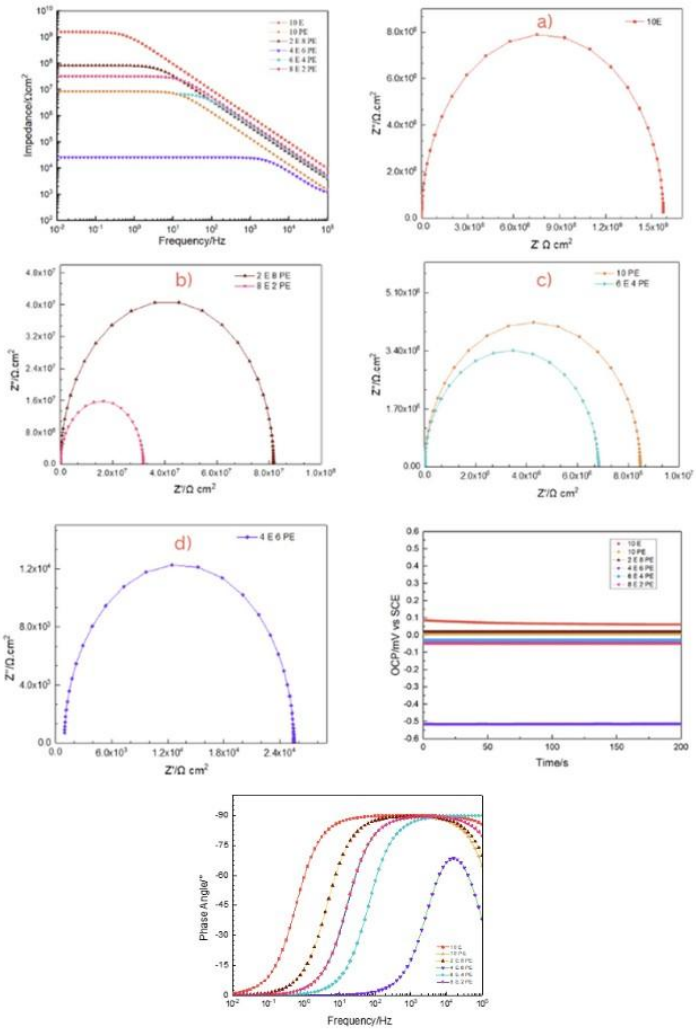


**Fig. 6. Day 1 EIS results of all samples.**

In contrast, the 4E6PE and 8E2PE samples presented notably smaller arcs with distorted or depressed profiles, symptomatic of irregular phase distribution and compromised barrier uniformity. The reduced arc radius and deviation from ideal capacitive behaviour in these systems are indicative of heterogeneities that facilitate localized charge transport and early-stage coating degradation, as supported by Zhang et al. [29].

Open Circuit Potential (OCP) measurements further validated these findings by evaluating the thermodynamic stability and corrosion tendency of each coating. The 10E coating demonstrated the most noble and stable potential (approaching 0 V vs. SCE), consistent with minimal electrochemical reactivity and strong surface passivation. Similarly, the 2E8PE and 10PE coatings maintained relatively stable and noble OCP values, indicative of low corrosion current density and sustained barrier performance. In contrast, the 4E6PE and 8E2PE samples exhibited more

negative and fluctuating OCP readings, suggesting that these systems were more susceptible to ionic ingress and corrosion initiation due to incomplete film coverage or interfacial weakness. According to Kumar et al. [6], such cathodic drift in early-stage OCP profiles reflects local disruption of the passive film and the early onset of corrosion reactions beneath the coating layer.

The phase angle response provides a complementary view of each system's dielectric performance across the frequency spectrum. The 10E coating displayed a high and broad phase angle plateau of approximately -85°, sustained over several decades of frequency, which is indicative of a nearly ideal capacitive response and minimal faradaic activity. This wide phase range reflects strong electrochemical insulation and confirms the presence of a highly coherent and crosslinked barrier. The 10PE and 2E8PE coatings also demonstrated relatively broad and elevated phase responses, reflecting favourable polarization behaviour, particularly due to PDMS-induced surface hydrophobicity and stable polymer dispersion. In contrast, the phase angle profiles of 4E6PE and 8E2PE were narrower and exhibited suppressed peaks, pointing toward increased ionic permeability and reduced capacitive resistance, likely due to internal microchannels or hydrophilic domains. As described by Qi et al. [27], this suppression is a hallmark of coatings with poor polymer chain interconnectivity or morphological weaknesses that allow water-induced relaxation and breakdown of dielectric properties.

In summary, the Day 1 EIS analysis establishes a clear hierarchy in corrosion resistance performance. The 10E formulation offers the most effective protection due to its dense crosslinked structure and high impedance characteristics. The 2E8PE hybrid and 10PE formulations also demonstrated promising early-stage performance, benefitting from hydrophobicity and adequate film uniformity. In contrast, the reduced electrochemical stability of 8E2PE and 4E6PE highlights the importance of achieving optimal resin compatibility, crosslink density, and morphological cohesion to prevent premature degradation. These results underscore the significance of precise formulation control in designing epoxy-based coatings for environments with aggressive ionic conditions.

The Day 10 plots offer critical insight into the intermediate-stage corrosion protection performance and degradation mechanisms of epoxy-polyester composite coatings following continuous immersion in 3.5 wt.% NaCl solution as shown in Fig. 7. Compared to the Day 1 measurements, clear performance shifts are observed, signalling the progressive evolution of the coating matrix under saline stress and the varying ability of each formulation to retain its barrier function over time.

The Bode plots reveal a noticeable reduction in the impedance modulus across all samples, particularly in the low-frequency region, which is widely regarded as a sensitive indicator of coating integrity and water barrier efficiency. The epoxy-rich 10E coating, while experiencing a measurable drop from its initial ($|Z|_{0.01\,Hz}$) exceeding $10^9\ \Omega\cdot cm^2$, still maintains the highest impedance ($10^8\ \Omega\cdot cm^2$), indicating sustained resistance to electrolyte diffusion. This retention is attributed to the intrinsic rigidity and crosslink density of the epoxy network, which delays microdefect formation and water uptake. Nonetheless, the decline suggests initial onset of polymer relaxation or microcrack initiation, as similarly described by Kumar et al. [6] in long-term epoxy barrier degradation studies.

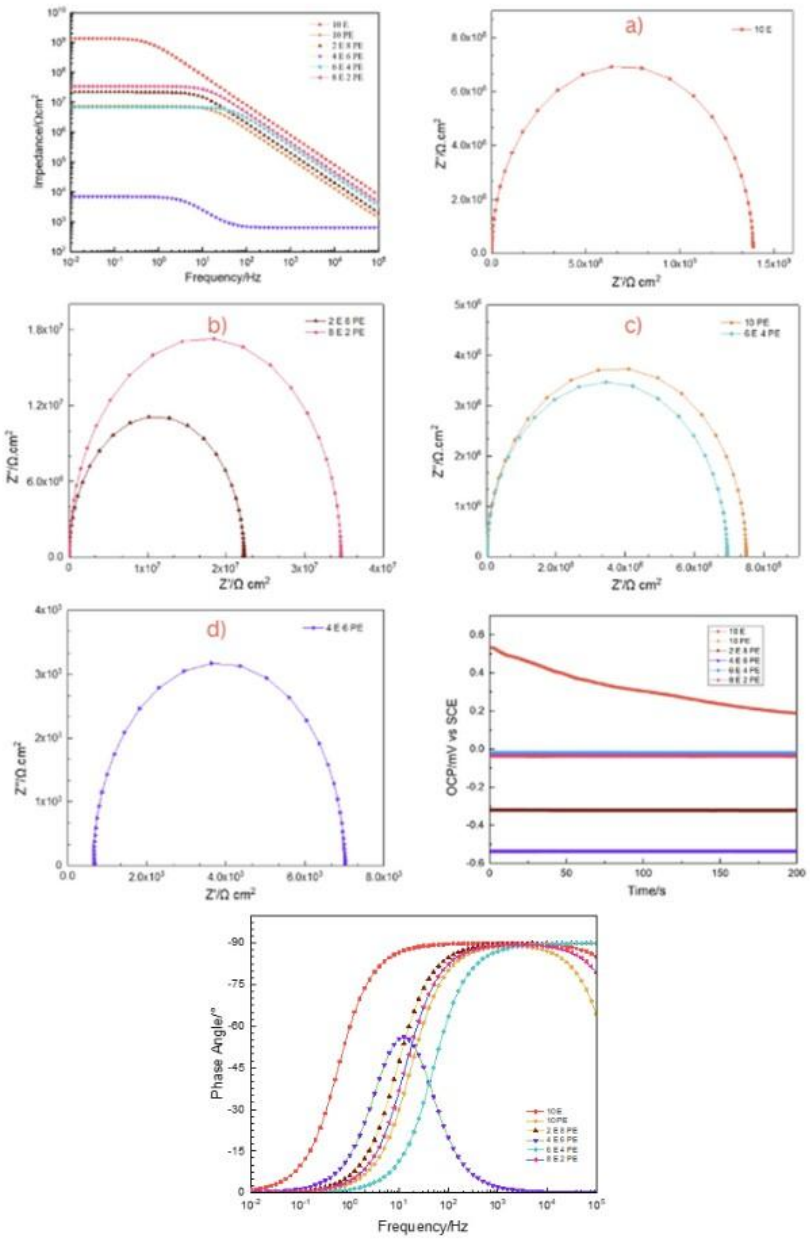


**Fig. 7. Day 10 of EIS results of all systems.**

The 10PE and 6E4PE formulations also show a moderate impedance decrease, maintaining performance in the $10^6$-$10^7$ Ω·cm² range. Their stability is likely aided by the presence of hydrophobic polyester backbones and PDMS-modified surfaces, which reduce surface energy and slow down water ingress. However, the most significant impedance decline is observed in the 8E2PE and 4E6PE coatings, with values falling

below $10^5\ \Omega \cdot cm^2$, indicating the emergence of substantial film degradation. These systems, which exhibited weaker phase compatibility and insufficient crosslinking on Day 1, now demonstrate pronounced susceptibility to moisture-induced defects, consistent with the degradation pathways reported by Zhang et al. [29], where unbalanced resin ratios led to early hydrolysis and under film corrosion.

The Nyquist plots further elucidate this electrochemical evolution. All systems display single semicircular arcs, denoting capacitive-dominant behaviour, though their arc diameters contract significantly compared to Day 1. The 10E coating retains the largest arc diameter, reaffirming its superior charge transfer resistance and structural coherence. However, the semicircle exhibits a slight flattening and lateral shift commonly attributed to rising solution resistance (Rs) and the formation of dielectric gradients within the partially wetted film. The 10PE and 6E4PE coatings also preserve relatively broad arcs, albeit with evident compression, suggesting reduced but still active resistance to interfacial charge movement. Conversely, the Nyquist plots of 8E2PE and 4E6PE are notably contracted and distorted, resembling depressed semicircles or sloped lines characteristic of Warburg impedance at low frequencies, signifying that ionic diffusion is beginning to dominate the corrosion process. As highlighted by Huang et al. [3] this behaviour is typical in coatings undergoing water-induced plasticization and microchannel formation, which increase permeability and reduce charge resistance.

Open Circuit Potential (OCP) profiles collected over 200 s offer thermodynamic evidence of these trends. The 10E sample continues to exhibit the most noble and stable potential (near 0 V vs. SCE), with only minor drift, suggesting sustained passivity and minimal anodic activity. Such stability implies a dense and adherent film capable of isolating the substrate from aggressive ionic species. The 10PE and 6E4PE coatings show moderately noble and steady potentials, reflecting ongoing suppression of electrochemical reactions at the metal interface. In contrast, 8E2PE and 4E6PE exhibit increasingly negative and unstable OCP trajectories, indicative of compromised surface protection and the initiation of localized corrosion. In other words, the declining OCP values correlated strongly with electrolyte penetration, interfacial swelling, and the early breakdown of film cohesion [6].

With respect to these findings, the phase angle plots provide insight into the dielectric performance and capacitive behaviour of each system. On Day 1, the 10E sample displayed a wide plateau near −85°, consistent with ideal capacitive response and negligible ionic transport. By Day 10, while the phase angle remains high, the plateau narrows and shifts slightly toward lower frequencies, which signalled the emergence of localized dielectric loss and moisture-induced relaxation within the polymer network. The 10PE and 6E4PE coatings similarly exhibit narrowing of the plateau and a moderate decrease in peak magnitude, indicating a partial transition toward resistive behaviour, though capacitive dominance is still evident. In stark contrast, the 8E2PE and 4E6PE samples display significantly suppressed peak values, with a sharp drop in phase angle and early-frequency crossover. These changes signify a substantial loss of insulating capability and the progression of the coatings toward a more conductive, porous state. Moreover, such phase suppression was identified as a reliable signal of coating failure due to water-induced dielectric collapse and breakdown of crosslinked domains.

In overall, the Day 10 electrochemical data illustrated a clear divergence in the mid-term performance of the tested coatings. The epoxy-based 10E formulation

maintains the highest level of protection, followed by the PDMS-enhanced 10PE and 6E4PE systems, which benefit from their hydrophobic surface properties and moderate film stability. By contrast, the 8E2PE and 4E6PE coatings reveal substantial degradation, underscoring the vulnerability of poorly crosslinked, phase-incompatible networks to accelerated corrosion in saline environments. These findings validate the critical role of crosslinking architecture, resin miscibility, and surface modification in determining not just initial coating efficacy, but also the ability to withstand progressive chemical and electrochemical stress. The observed changes across all four electrochemical metrics impedance, Nyquist arc radius, OCP shift, and phase angle suppression collectively support a holistic understanding of mid-term degradation dynamics and provide a robust framework for optimizing future coating formulations.

The EIS results obtained on Day 30 provide a comprehensive assessment of the long-term corrosion resistance of the developed epoxy composite coatings following immersion in 3.5 wt.% NaCl solution as shown in Fig. 8. As evidenced by the Bode plots, all formulations experienced a progressive decline in impedance magnitude over time, particularly within the low-frequency region, which is a critical indicator of coating barrier efficiency. This reduction signifies the cumulative effects of ionic permeation and water absorption, which compromise the dielectric properties of the coatings. Among all samples, the 10E formulation retained the highest 〖|Z|〗_(0.01 Hz) of approximately $10^8\,\Omega\cdot cm^2$, though reduced from its initial value ($>10^9\,\Omega\cdot cm^2$), demonstrating sustained barrier integrity even after prolonged exposure.

This continued performance is attributed to the dense crosslinked epoxy architecture that inhibits diffusion pathways, as reported by Motlatle et al. [28] , who reported long-term dielectric resilience in epoxy networks with high structural cohesion. The 8E2PE sample, previously observed to exhibit robust intermediate-term performance, also maintained a relatively high impedance profile, validating the effectiveness of its semi-balanced formulation in impeding ion transport. In contrast, the 4E6PE and 10PE coatings recorded the most pronounced impedance drops, indicative of advanced degradation mechanisms such as microcrack propagation, plasticization, and water-induced matrix swelling.

The corresponding Nyquist plots reinforce these findings by reflecting reduced charge transfer resistance (Rct) across the coating-substrate interface. All systems displayed contracted semicircular arcs relative to earlier immersion stages, signifying a decrease in polarization resistance. Despite this, the 10E sample remained dominant, retaining the widest arc and thereby confirming its superior corrosion resistance. The 8E2PE coating surpassed 2E8PE in arc diameter, suggesting improved resistance attributed to a more favourable polymeric network structure and enhanced PDMS dispersion that delays electrolyte ingress. These improvements imply that an epoxy-rich phase with sufficient compatibility and surface modification can synergistically extend electrochemical stability.

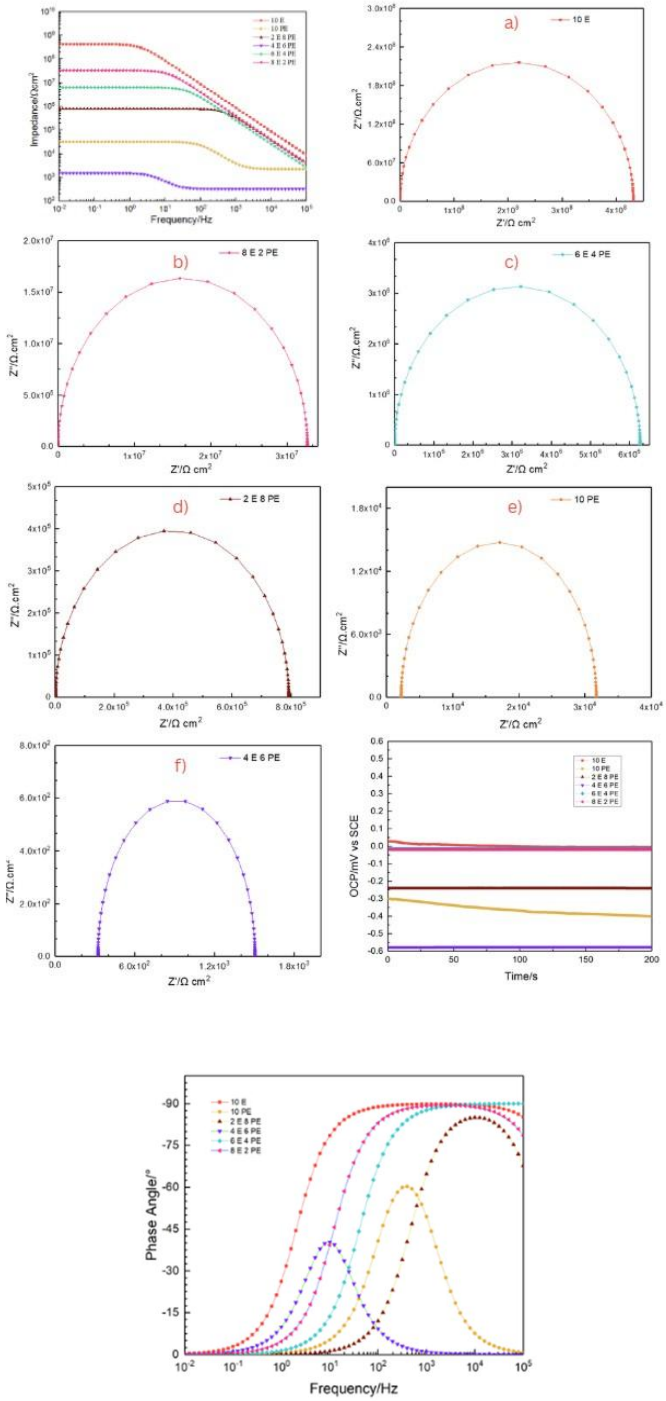


**Fig. 8. Day 30 EIS results of all samples.**

Conversely, the arcs for 10PE and 4E6PE nearly collapsed, approaching the origin and indicating minimal interfacial resistance - a condition symptomatic of electrolyte saturation and initiation of underfilm corrosion. The increasing offset of semicircle origins from (0,0), consistent across all samples and more prominent by Day 30, suggests the formation of a porous diffusion layer at the interface. Furthermore,, such displacements are diagnostic of weakening coating adhesion and the evolution of ionic transport channels due to matrix degradation [24].

The OCP profiles further substantiated these interpretations, offering insight into the thermodynamic stability and corrosion kinetics of each coating system. The 10E coating continued to exhibit the most noble and stable OCP values, remaining close to 0 V vs. SCE, reflecting minimal anodic activity and effective barrier continuity. This observation is consistent with the presence of a well-sealed coating-metal interface, which resists electrochemical reactions. The 8E2PE formulation showed a moderate negative shift but maintained relative stability, indicating partial retention of its protective properties. In contrast, 10PE and 4E6PE exhibited increasingly negative and fluctuating OCP trends, highlighting their reduced ability to suppress electrochemical activity and their susceptibility to localized corrosion. These behaviours mirror the findings of Kumar et al. [6], who emphasized that declining OCP readings are reliable indicators of underfilm corrosion and progressive barrier failure due to poor crosslink density and elevated moisture absorption.

The phase angle plots offer additional dielectric characterization of each coating. The 10E sample retained a broad plateau near −80°, although slightly narrowed compared to earlier stages, signifying a reduction in dielectric homogeneity but still maintaining a capacitive response indicative of a well-insulated system. Similarly, 8E2PE demonstrated a reasonably stable phase angle profile, with a peak nearing −70°, reflecting its semi-capacitive nature and effective suppression of ion transport due to PDMS inclusion and partial epoxy dominance. By contrast, both 10PE and 4E6PE exhibited severely diminished phase peaks (below −40°) and narrowed plateaus, denoting substantial deterioration of the dielectric layer. This suppression is characteristic of coatings that have transitioned from capacitive to resistive or diffusive behaviour due to internal pore development and polymer matrix degradation. As reported by Kumar et al. [6], phase angle narrowing and leftward peak shifts are typical of coatings undergoing microchannel formation and electrochemical instability arising from inadequate molecular cohesion and excessive water uptake.

Collectively, the Day 30 electrochemical profiles validate the hypothesis that the long-term corrosion resistance of epoxy composite coatings is governed by their crosslinking architecture, resin phase compatibility, and surface hydrophobicity. While all coatings experienced degradation under extended saline exposure, the epoxy-dominant 10E formulation exhibited the highest level of sustained performance, attributed to its dense molecular structure and high interfacial adhesion. The 8E2PE hybrid coating, despite moderate impedance loss, demonstrated promising long-term protection, outperforming several other blends due to a favourable balance between epoxy rigidity and PDMS-induced hydrophobicity. Conversely, polyester-rich systems such as 10PE and 4E6PE failed to preserve their electrochemical stability, largely due to inferior crosslinking, greater water permeability, and microstructural weaknesses. These findings are in alignment with long-term degradation models in literature and underscore the

critical importance of rational formulation design, particularly in optimizing epoxy concentration and surface modification strategies, to ensure durable corrosion resistance in aggressive marine and industrial environments.

## 5. Conclusions

The experimental results presented in this study affirm that the strategic blending of epoxy resin with a controlled fraction of polyester augmented by the incorporation of PDMS and carefully selected curing agents yields composite coatings with markedly improved functional performance relative to monomeric systems. Among all formulations evaluated, the 8E2PE composition emerged as the most effective, exhibiting a well-balanced integration of electrochemical durability, cohesive adhesion, and surface hydrophobicity. This optimized hybrid formulation maintained consistently high impedance values across all EIS assessments, even after 30 days of continuous immersion in 3.5 wt.% NaCl solution. Its performance was further validated by a broad phase angle plateau, stable OCP, and minimal charge transfer activity in Nyquist plots, collectively confirming the formation of a resilient barrier film. In addition, the 8E2PE coating achieved a perfect adhesion rating (5B) and presented favourable WCA results, underscoring its robust interfacial cohesion and moisture repellence.

These findings reflect the synergistic effects of combining the high crosslinking density and mechanical integrity of epoxy resin with the flexibility and surface energy modulation afforded by polyester and PDMS, respectively. In contrast, coatings with elevated polyester content such as 10PE and 4E6PE exhibited substantial degradation over time, including reduced impedance, negative OCP shifts, compromised adhesion, and decreased WCA values. These deficiencies can be attributed to the lower crosslink density, limited polar functionality for substrate interaction, and less efficient phase compatibility inherent in polyester-dominant matrices. The observed differences across formulations emphasize the critical role of polymer miscibility, curing kinetics, and phase uniformity in determining long-term corrosion resistance and mechanical performance.

The successful implementation of the 8E2PE system exemplifies how hybrid resin architectures can be engineered to achieve multifunctional performance, balancing mechanical robustness with environmental resistance. This approach represents a significant advancement in the design of high-performance protective coatings, particularly for applications in marine, offshore, and industrial sectors where prolonged exposure to aggressive environments necessitates superior material resilience. Ultimately, the findings contribute meaningfully to the existing body of literature on corrosion-resistant polymeric coatings, providing both empirical evidence and mechanistic insight into the development of next-generation epoxy-based composite systems. The demonstrated potential of epoxy–polyester–PDMS hybrids paves the way for scalable, cost-effective, and sustainable solutions in advanced surface protection technologies.

## References

1. Koch, G.H.; Brongers, M.P.H.; Thompson, N.G.; Virmani, Y.P.; and Payer, J.H. (2001). Corrosion cost and preventive strategies in the United States. *Federal Highway Administration* (*FHWA*), *FHWA-RD-01-XXX.*

2. Yang, W.; Feng, W.; Liao, Z.; Yang, Y.; Miao, G.; Yu, B.; and Pei, X. (2021). Protection of mild steel with molecular engineered epoxy nanocomposite coatings containing corrosion inhibitor functionalized nanoparticles. *Surface and Coatings Technology*, 406, 126639.
3. Huang, B.; Zhang, C.; Zhang, G.; and Liao, H. (2019). Wear and corrosion resistant performance of thermal-sprayed Fe-based amorphous coatings: A review. *Surface and Coatings Technology*, 377, 124896.
4. Adnan, S.N.A.; Kahar, N.E.A.; Sobari, M.S.; Mohamed, S.H.; Chen, L.J.; Lee, E.; Pargi, M.N.F.; and Musa, M.S. (2025). Effect of epoxy content on the corrosion properties of waterborne epoxy-acrylate coating. *Journal of Coatings Technology and Research*, 2025.
5. Kumar, S.S.A.; Ramesh, K.; Ramesh, S.; Ramesh, S.; and Bang, L.T. (2024). A study on hybrid composite coatings: The significance of its surface wettability, dispersibility and thermal degradation performances. *Progress in Organic Coatings*, 189, 108351.
6. Kumar, S.S.A.; Ramesh, K.; and Ramesh, S. (2025). Enhancement of barrier protection of organic coatings with the incorporation of graphene oxide as a reinforcing filler. *Current Applied Physics*, 73, 98-111.
7. Peng, Z.; Zhu, A.; and Zhang, T. (2024). The novel preparation of waterborne acrylic polyurethane-silica organic-inorganic interpenetrating network coatings. *Progress in Organic Coatings*, 187, 108157.
8. Aktas, C.; Polat, O.; Beitollahpoor, M.; Farzam, M.; Pesika, N.S.; and Sahiner, N. (2023). Force-based characterization of the wetting properties of LDPE surfaces treated with $CF_4$ and $H_2$ plasmas. *Polymers*, 15(9), 2132.
9. Joy, J.; Winkler, K.; Bassa, A.; Vijayan P, P.; Jose, S.; Anas, S.; and Thomas, S. (2023). Miscibility, thermal degradation and rheological analysis of epoxy/MABS blends. *Soft Matter*, 19(1), 80-89.
10. Kumar, S.S.A.; Wonnie Ma, I.A.; Ong, G.; Ramesh, K.; and Ramesh, S. (2023). An insight on the corrosive performance of acrylic-epoxy based coatings: the significance of its electrochemical impedance evaluations. *Journal of Polymer Research*, 30(6), 200.
11. Cakmak, M.; and Greener, J. (2023). *Polyester Films: Materials, processes and applications*. Wiley.
12. Hexion. (2021). Technical data sheet. Retrieved October 5, 2025, from chrome-extension://efaidnbmnnnibpcajpcglclefindmkaj/https://www.penpoly.com/app/uploads/2021/07/Epikure-3388_tds.pdf
13. Li, D.; Yu, L.; Lu, Z.; Kang, H.; Li, L.; Zhao, S.; Shi, N.; and You, S. (2024). Synthesis, structure, properties, and applications of fluorinated polyurethane. *Polymers*, 16(7), 959.
14. Chawla, K.K. (1998). *Composite materials: Science and engineering*. Springer.
15. Kumar, S.S.A.; Wonnie Ma, I.A.; Ong, G.; Ramesh, K.; and Ramesh, S. (2024). The synergistic effects of graphene on the physical, hydrophobic, surface, and thermal properties of acrylic-epoxy-polydimethylsiloxane composite coatings. *International Journal of Adhesion and Adhesives*, 128, 103546.
16. Stuart, B.H. (2004). *Infrared spectroscopy*: *Fundamentals and applications*. John Wiley & Sons.

17. Wiley. (2008). *Characterization and analysis of polymers*. John Wiley & Sons.
18. Saikia, M.; Dutta, T.; Jadhav, N.; and Kalita, D.J. (2025). Insights into the development of corrosion protection coatings. *Polymers*, 17(11), 1548.
19. Bratasyuk, N.A.; Latyshev, A.V.; and Zuev, V.V. (2023). Water in epoxy coatings: Basic principles of interaction with polymer matrix and the influence on coating life cycle. *Coatings*, 14(1), 54.
20. Samad, U.A.; Alam, M.A.; Anis, A.; Sherif, E.-S.M.; Al-Mayman, S.I.; and Al-Zahrani, S.M. (2020). Effect of incorporated ZnO nanoparticles on the corrosion performance of $SiO_2$ nanoparticle-based mechanically robust epoxy coatings. *Materials*, 13(17), 3767.
21. Kwok, D.; and Neumann, A. (1999). Contact angle measurement and contact angle interpretation. *Advances in Colloid and Interface Science*, 81(3), 167-249.
22. ASTM International. (2023). Standard test methods for measuring adhesion by tape test. Retrieved October 5, 2025, from https://store.astm.org/d3359-23.html
23. Barsoukov, E.; and Macdonald, J.R. (2018). *Impedance spectroscopy*: *Theory, experiment, and applications*. John Wiley & Sons, Inc.
24. Neves, L.B.; Afonso, I.S.; Nobrega, G.; Barbosa, L.G.; Lima, R.A.; and Ribeiro, J.E. (2024). A review of methods to modify the PDMS surface wettability and their applications. *Micromachines*, 15(6), 670.
25. Ramos, I.; Gonçalves, M.; Gonçalves, I.M.; Carvalho, V.; Fernandes, E.; Lima, R.; and Pinho, D. (2025). PDMS surface wettability modification and its applications: A systematic review. *Journal of Molecular Liquids*, 127978.
26. Pistone, A.; Scolaro, C.; and Visco, A. (2021). Mechanical properties of protective coatings against marine fouling: A review. *Polymers*, 13(2), 173.
27. Qi, D.; Zhang, K.; Tian, G.; Jiang, B.; and Huang, Y. (2021). Stretchable electronics based on PDMS substrates. *Advanced Materials*, 33(6), 2003155.
28. Motlatle, A.M.; Ray, S.S.; Ojijo, V.; and Scriba, M.R. (2022). Polyester-based coatings for corrosion protection. *Polymers*, 14(16), 3413.
29. Zhang, X.; Dong, M.; Cai, X.; Chen, D.; Xian, Y.; Zheng, X.; Guo, Z.; and Algadi, H. (2023). Progress in machining-induced residual stress and microstructural evolution of inhomogeneous materials and composites. *Advanced Composites and Hybrid Materials*, 6(3), 122.